An Evaluation of the ICM Algorithm for Image Reconstruction

R. H. GLENDINNING

School of Mathematical Sciences,University of Bath, Bath BA2 7AY, U.K.

We examine the properties of Iterated Conditional Modes (ICM) estimation for a number of synthetic binary images using simulation.

KEY WORDS : *Ill-posed problem;image reconstruction;ICM; Simulated Annealing;smoothing parameter; neighbourhood system;Monte-Carlo.*

1. INTRODUCTION

In the last few years considerable interest has been shown in the problems posed by the analysis of images corrupted by random noise. The reconstruction of such images leads to special difficulties as it is an ill-posed problem (in the sense described by O'Sullivan, 1986). Typically the reconstruction of an array of pixels will have as many parameters as observations. A number of techniques have been proposed which *solve* ill-posed problems by restricting the class of admissible solutions,see Marroquin,Mitter & Poggio (1987). This is achieved by introducing a priori knowledge about admissible solutions.

Much interest currently centres on techniques which incorporate knowledge about the underlying image using Bayesian methodology, See Geman & Geman (1984) ; Kashyap & Lapsa (1984). These techniques assume that the underlying scene can be adequately described as a realisation from a prescribed Markov random field. Motivated by this approach Besag (1986) introduced a technique known as **ITERATED CONDITIONAL MODES (ICM).** This iterative procedure incorporates knowledge about the underlying scene by the choice of a 'neighbourhood system' ,weight function and smoothing parameter. Broadly

speaking this method exploits the tendency of adjacent pixels to have the same colour. A similar approach based on spatial auto regression is described in Woods,Dravida & Mediavilla (1987).

In this paper we use simulation to evaluate the performance of ICM in reconstructing binary (black-white) images. The reconstruction of binary images is of considerable practical importance as many problems in object recognition and manipulation fall into this category. For simplicity we suppose that the underlying scene can be partitioned into an array of pixels (picture elements) which are *uniquely* coloured black or white. At each pixel we observe a signal which depends on its colour. We consider the case where each signal is additively corrupted by independent normally distributed noise. These are highly unrealistic assumptions as they ignore the problems associated with mixed pixels, signal spread etc. However we believe that the study of ICM in this simplified setting will give valuable insight into its behaviour in more complex situations.

In section 2 we describe the basic ICM algorithm and recall some basic facts about Markov random fields. The synthetic scenes used in this study are described in section 3. In section 4 we examine the influence of the neighbourhood system and weight function on the quality of our reconstructions. The choice of smoothing parameter is discussed in section 5. We are particularly interested in identifying properties of the underlying scene which influence the value given to β (the smoothing parameter). Some distributional properties of ICM reconstructions are discussed in section 6. The numerical performance of the basic ICM algorithm is discussed in section 7. We describe several modifications of the basic algorithm which enhance its efficiency. Our findings are summarised in section 8.

The problem of restoring corrupted images has a long history in the image processing literature, where a number of techniques of varying sophistication have been suggested, see Bovik,Huang & Munson (1987) or Rosenfeld & Kak (1982). A comparison of ICM with the multitude of competing techniques is

not attempted in this paper.

2. THE ICM ALGORITHM AND MARKOV RANDOM FIELDS

Let W be a rectangular window in the plane which is partitioned into an $(m \ x \ n)$ array of rectangular pixels of equal size. We assume that each pixel can be uniquely coloured. The available colours are labelled $(1,2,...,c)$. In this paper we restrict attention to scenes with two colours which we call black and white. The colour of the $(i,j)^{th}$ pixel is denoted by x_{ij}. We refer to (x_{ij}) as the true or underlying scene. Suppose we observe an array of signals (y_{ij}) generat-

$$y_{ij} = \mu(x_{ij}) + \varepsilon_{ij}, \tag{2.1}$$

where (ε_{ij}) are independent and identically distributed random variables and $\mu(.)$ is a function of x_{ij} only. The object of image analysis is to estimate the true or underlying scene (x_{ij}) from (y_{ij}). In this paper we consider real-valued signals only. Models of this form are not canonical in the study of corrupted images and the reader is referred to Besag (1986) for a discussion of alternative models.

At first sight the natural way of estimating (x_{ij}) is by maximum likelihood. In this approach we find (x_{ij}) which maximises

$$l(\,(y_{ij}) \mid (x_{ij})\,) = \prod_{i=1}^{m}\prod_{j=1}^{n} f\,(y_{ij} \mid x_{ij}). \tag{2.2}$$

where $f\,(y_{ij} \mid x_{ij})$ is the fully specified density function of y_{ij} conditional on x_{ij}. The estimates produced by this approach are usually unsatisfactory as (2.1) has as many parameters (x_{ij}) as observations. To improve the situation Geman & Geman (1984) and Besag (1986) introduce information about (x_{ij}) into the estimating procedure. This is achieved by regarding (x_{ij}) as a realisation from a **Markov random field (MRF)** . A detailed account of the salient features of MRF's can be found in Geman & Geman (1984) ; Besag (1974,1986) or Suomela (1976). We briefly outline the main properties of MRF's relevant to

the discussions in this paper.

For each pixel (i,j) we associate a set of pixels $F_{(i,j)}$, not including (i,j) called the **neighbourhood** of (i,j). The collection of sets $(F_{(i,j)})$ is called a neighbourhood system and satisfies the condition : $(p,q) \in F_{(i,j)} \Leftrightarrow (i,j) \in F_{(p,q)}$.

Then (x_{ij}) is a MRF **if**

(1) $P(x_{ij} \mid (x_{pq}, p \neq i, q \neq j)) = P(x_{ij} \mid x_{pq}, (p,q) \in F_{(i,j)})$,

(2) $P((x_{ij})) > 0$,

where $P((x_{ij}))$ is the probability associated with the realisation (x_{ij}). Conditions 1 and 2 impose severe restrictions on $P(.)$. Valid forms of $P(.)$ are given by the Hammersley-Clifford Theorem, see Besag (1974) or Suomela (1976).

We follow Geman & Geman (1984) and adopt a Bayesian approach where we estimate (x_{ij}) from its posterior distribution

$$l((y_{ij}) \mid (x_{ij}))P((x_{ij})). \tag{2.3}$$

A plausible estimate of (x_{ij}) is the value of (x_{ij}) which maximises (2.3). This is the MAP estimate of (x_{ij}). Geman & Geman (1984) use simulated annealing to maximise (2.3). Van Laarhoven & Aaris (1987) give a comprehensive description of simulated annealing and its application to image analysis. Note that Greig,Porteous and Seheult, in the discussion of Besag (1986) show that the MAP estimate of a binary scene can be calculated exactly. It is not known whether the MAP estimator has any desirable properties in this context.

Besag (1986) introduces an alternative estimator of (x_{ij}) known as **ITERATED CONDITIONAL MODES (ICM).** This algorithm converges to a local maximum of (2.3). Let $(\hat{x}_{ij})$ be the current estimate of (x_{ij}). For each pixel we find the value of x_{ij} which maximises

$$f(y_{ij} \mid x_{ij})P(x_{ij} \mid (\hat{x}_{ij})), \tag{2.4}$$

where $P(x_{ij} \mid (\hat{x}_{ij}))$ depends on the neighbours of (i,j) only. Consider an exam-

ple. Let (x_{ij}) be a binary scene and (ε_{ij}) an array of independent normally distributed random variables with zero mean and variance σ^2. We represent our knowledge of (x_{ij}) by a MRF with neighbourhood system $(F_{(i,j)}=((i-1,j),(i+1,j),(i,j-1),(i,j+1)))$ and conditional probabilities

$$P(x_{ij}=k \mid (x_{pq}p \neq i, q \neq j)) = \frac{\exp(\beta u_{ij}(k))}{\exp(\beta u_{ij}(0)) + \exp(\beta u_{ij}(1))}, \quad k=0,1, \qquad (2.5)$$

where the weight function $u_{ij}(k)$ is the number of neighbours of x_{ij} with colour k. The value of x_{ij} which maximises (2.4) minimises

$$(2\sigma^2)^{-1}(y_{ij} - \mu(x_{ij}))^2 - \beta\hat{u}_{ij}(x_{ij}), \qquad (2.6)$$

where $\hat{u}_{ij}(x_{ij})$ is the number of neighbours of (i,j) which have colour x_{ij} under the current estimate $(\hat{x}_{ij})$. We call β the smoothing parameter. The extension of (2.6) to non-gaussian noise is immediate.

Notice that (2.6) is in the form of a penalised likelihood and may be interpreted in this way without recourse to Bayesian arguments. Note that ICM and MAP are not equivalent for most scenes. Typically smaller values of β (relative to ICM) are required for MAP, see Greig,Porteous and Seheult,in the discussion of Besag (1986). The relationship between techniques like ICM and other regularisation procedures is discussed in Titterington (1985).

3. DESCRIPTION OF THE SIMULATION STUDY

Seven scenes of varying complexity were constructed by partitioning the unit square into 10^4 square pixels of equal size. The colour of each pixel was assigned to the colour of its mid-point. In this study we use black and white scenes only.

To identify properties of ICM more easily we restrict attention to simple synthetic scenes which cover a small alphabet of forms rather than use naturally occurring images. Five simple geometric scenes are displayed in figures 1 to 5. The remaining scenes, MRF2 and MRF3 (figures 6 and 7) are realisations

from a Markov random field with *prescribed* number of black pixels (approx 50%). MRF2 and MRF3 were constructed using the algorithm described in Cross & Jain (1983). Notice that we are sampling from the *conditional* distribution of the prescribed MRF. We believe that realisations constructed in this way capture much of the local structure of the *unconditional* model. In the next section we describe three Markov random fields, (Models I,II and III) which are commonly used in this context. MRF2 is drawn from Model II with β=0.5 and MRF3 from Model III with β=0.75.

We construct an array of signals (y_{ij}) using (2.1) with $\mu(black)=1$, $\mu(white)=0$ and (ε_{ij}) an array of independent normally distributed random variables with zero mean and variance σ^2. The maximum likelihood reconstruction is calculated and used as the initial state for the ICM algorithm. This iterative procedure is terminated after twelve iterations. Typically convergence occurs after six iterations. This process is repeated fifteen times for each combination of parameter and underlying model. The efficiency of this algorithm is discussed in section 7.

Many criteria can be used to evaluate reconstructions. Essentially its choice depends on the image characteristics of greatest interest. In this paper we use the number of misclassified pixels as an appropriate measure. The suitability of this criteria has been the subject of much recent debate, see the discussion of Besag (1986). We point out the limitations of this criteria where appropriate.

Figs 1-7 here

4. THE CHOICE OF MODEL.

In this section we examine the effect of choosing three different weight functions in (2.6). The choice of β is discussed in section 5. In a Bayesian framework we are modelling our knowledge of the uncorrupted scene by a MRF with prescribed structure. Cross & Jain (1983) show that simple MRF's can

generate a wide variety of binary scenes. The problem of choosing suitable MRF's to model specific scenes is not well understood,see Kashyap & Chelappa (1983) , Enting & Welberry (1978) and Pickard (1987). The last two authors discuss parameter estimation for Markov random fields. An additional complication arrises when our knowledge about the underlying scene is imprecise or difficult to model by a MRF. The success of this approach rests on the assumption that only certain modest properties of our 'prior' are important. Some tentative observations on the robustness of ICM reconstruction to model specification are given in sections 4 and 5.

In this section we use three different MRF's to describe our knowledge about the scenes presented in figs 1 to 7. We examine the misclassification rate achieved by ICM using each model and several values of the parameter β. The models used are as follows:

MODEL I : A first order neighbourhood.

$$F_{(i,j)} = (\ (i-1,j),(i+1,j),(i,j+1),(i,j-1)\ ).$$

$$P(x_{ij}=k \mid F_{(i,j)}) = \frac{\exp(\beta u_{ij}(k))}{\exp(\beta u_{ij}(0)) + \exp(\beta u_{ij}(1))},\ k=0,1. \tag{4.1}$$

where

$$u_{pq}(k) = 1 \quad , \quad when \quad (p,q) \in F_{(i,j)} \text{ and } x_{pq} = k, \tag{4.2}$$

and zero otherwise.

MODEL II: A second order neighbourhood.

$$F_{(i,j)} = (\ (i-1,j+1),(i+1,j+1),(i-1,j-1),(i+1,j-1),$$
$$(i-1,j),(i,j+1),(i+1,j),(i,j-1))$$

$P(x_{ij}=k \mid F_{(i,j)})$ is given by (4.1) and (4.2).

MODEL III : As for II with down weighted diagonals. $F_{(i,j)}$ as for the previous model and $P(x_{ij}=k \mid F_{(i,j)})$ given by (4.1) with

$$u_{pq}(k) = 1 \quad , (p,q) \in ((i+1,j),(i-1,j),(i,j+1),(i,j-1)) \text{ and } x_{pq} = k.$$

$$u_{pq}(k) = 2^{-1/2} \quad , (p,q) \in ((i-1,j+1),(i+1,j-1),(i+1,j+1),(i-1,j-1)) \text{ and } x_{pq} = k.$$

$$u_{pq}(k) = 0 \ \textit{otherwise}. \tag{4.3}$$

There are conflicting opinions as to whether models should be modified for pixels adjacent to the window,see Ripley (1984). In this study we use the unmodified models I,II and III. The effects of modification appear small relative to the standard errors encountered in this study. Cross & Jain (1983) show that models like I,II and III can be used to construct a wide variety of binary scenes.

TABLE I

Comparison of models I, II and III
Smallest average percentage of misclassified pixels
β taking values in (0.25,0.5,0.75,1.0,1.25,1.5) for Models II and III
β taking values in (0.5,1.0,1.5,2.0,2.5,3.0) for Model I
The standard error of this estimate is given in brackets

$\sigma^2 = 0.5$			ML	15.87		
			Model			
Picture	I		II		III	
BCIR	2.24	(0.07)	0.55	(0.04)	0.60	(0.04)
CROSS	2.66	(0.05)	1.00	(0.07)	0.98	(0.06)
TWO	2.40	(0.09)	1.11	(0.05)	0.97	(0.06)
MANY	3.94	(0.10)	2.41	(0.07)	2.27	(0.08)
VMANY	8.40	(0.13)	7.11	(0.10)	7.24	(0.10)
MRF3	6.81	(0.07)	4.92	(0.09)	4.98	(0.10)
MRF2	9.50	(0.14)	7.85	(0.09)	7.98	(0.09)

$\sigma^2 = 1.0$			ML	30.85		
			Model			
Picture	I		II		III	
BCIR	6.33	(0.16)	1.32	(0.07)	1.32	(0.05)
CROSS	6.85	(0.22)	2.07	(0.12)	2.04	(0.10)
TWO	6.88	(0.13)	2.55	(0.08)	2.41	(0.08)
MANY	8.84	(0.15)	4.52	(0.16)	4.55	(0.12)
VMANY	15.11	(0.22)	13.44	(0.13)	12.92	(0.17)
MRF3	12.13	(0.16)	8.16	(0.19)	8.09	(0.17)
MRF2	14.92	(0.20)	11.40	(0.23)	11.34	(0.22)

Each scene described in figs 1 to 7 is reconstructed using models I,II and III with various values of σ^2 and β. For models II and III we find the value of β in the set (0.25,0.5,0.75,1.0,1.25,1.50) which gives the smallest average misclassification rate. For model I we consider values of β in the set (0.5,1.0,1.5,2.0,2.5,3.0). We choose different values of β for model I as there is strong empirical evidence that the 'optimal' value of β lies in this range for the scenes considered. In Table I we display the smallest average misclassification rate for $\sigma^2 = 0.5$ and 1.0 . Similar results were obtained using different values of σ^2. Notice that ICM is superior to the ML estimate for all scenes. It is readily apparent that model I is vastly inferior to II and III for all scenes considered. Model III is marginally superior to model II in the majority of cases (9 from 14). In their study of edge penalties Brown and Silverman (1987) present an argument which supports the use of model III in preference to Model II for the majority of scenes. Recall that MRF2 and MRF3 are realisations from a Markov random field with a fixed number of black pixels. Using the 'correct' model for these scenes appears to have little effect on the quality of the reconstruction.

As the 'optimal' β will usually be unknown we examine the average misclassification rates for model II and III for several values of β. The average percentage of misclassified pixels is presented in Tables II to VII for various values of β.

In Tables II and III we display the average percentage of misclassified pixels using models II and III for various values of β and σ^2=0.5. Similar results were obtained for other values of σ^2. There is strong evidence to suggest that the 'optimal' value of β using model III is larger than the corresponding value for model II. In figure 15 we compare the average percentage of misclassified pixels when MRF3 is reconstructed using models II and III (σ^2=0.5). We plot the average percentage of misclassified pixels using model II against β. For Model III we plot the corresponding percentage against $(1/1.17)\beta$. From this figure we see that a useful first approximation is to multiply the value of β used

with model II by 1.17 when using model III. This ensures that the second term in (2.6) has the same value for both models when $\hat{u}_{ij}(x_{ij})=8$.

TABLE II

Average percentage of misclassified pixels using Model II
Standard errors in brackets
Optimal reconstruction is bold faced

$\sigma^2 = 0.5$

β	BCIR	CROSS	TWO	MANY	VMANY	MRF2	MRF3
0.25	4.53	4.75	4.96	5.91	9.78	9.86	7.74
	(0.10)	(0.11)	(0.09)	(0.13)	(0.09)	(0.14)	(0.12)
0.50	0.80	1.02	1.30	**2.41**	**7.11**	**7.85**	**4.92**
	(0.03)	(0.04)	(0.04)	(0.07)	(0.10)	(0.09)	(0.09)
0.75	**0.55**	**1.00**	**1.11**	2.48	8.04	8.44	5.13
	(0.04)	(0.07)	(0.05)	(0.09)	(0.19)	(0.10)	(0.07)
1.00	0.63	1.01	1.20	2.53	9.56	9.01	5.48
	(0.04)	(0.05)	(0.07)	(0.09)	(0.18)	(0.09)	(0.08)
1.25	0.75	1.22	1.44	3.19	11.60	9.83	6.16
	(0.05)	(0.08)	(0.10)	(0.10)	(0.25)	(0.12)	(0.12)
1.50	0.70	1.27	1.78	3.61	13.19	10.40	6.77
	(0.03)	(0.08)	(0.12)	(0.12)	(0.28)	(0.13)	(0.12)

TABLE III

Average percentage of misclassified pixels using model III
Standard errors in brackets. Optimal reconstruction is bold faced

$\sigma^2 = 0.5$

β	BCIR	CROSS	TWO	MANY	VMANY	MRF2	MRF3
0.25	6.31	6.54	6.71	7.58	11.02	11.12	9.20
	(0.12)	(0.13)	(0.12)	(0.13)	(0.09)	(0.14)	(0.12)
0.50	1.18	1.38	1.59	2.78	**7.24**	**7.98**	5.22
	(0.05)	(0.05)	(0.06)	(0.07)	(0.10)	(0.09)	(0.09)
0.75	**0.60**	1.01	1.08	2.38	7.37	8.01	**4.98**
	(0.04)	(0.07)	(0.05)	(0.09)	(0.15)	(0.11)	(0.10)
1.00	0.64	**0.98**	**0.97**	**2.27**	8.26	8.63	5.20
	(0.04)	(0.06)	(0.06)	(0.08)	(0.19)	(0.08)	(0.09)
1.25	7.11	1.08	1.25	2.81	9.76	9.25	5.72
	(0.04)	(0.06)	(0.09)	(0.08)	(0.25)	(0.11)	(0.09)
1.50	6.87	1.08	1.44	3.13	11.24	9.72	6.22
	(0.04)	(0.08)	(0.09)	(0.11)	(0.30)	(0.12)	(0.11)

In Tables IV to VII we present the analogous results for black and white pixels. These results are similar to those in Tables II and III. Notice that the 'optimal' value of β is larger for white pixels than for black in the majority of scenes. This may be due to the higher proportion of boundary pixels for black

features in most scenes (see Table IX).

TABLE IV

Average percentage of black pixels classified white using model II
Standard errors in brackets.
Optimal reconstruction is bold faced

$\sigma^2=0.5$

β	BCIR	CROSS	TWO	MANY	VMANY	MRF2	MRF3
0.25	4.43	7.72	7.59	**11.91**	**16.16**	9.51	7.70
	(0.15)	(0.34)	(0.28)	(0.39)	(0.33)	(0.20)	(0.18)
0.50	0.77	**4.30**	**4.87**	12.13	18.46	**7.87**	**4.98**
	(0.06)	(0.41)	(0.21)	(0.44)	(0.48)	(0.16)	(0.12)
0.75	0.42	5.36	5.33	14.80	24.96	8.11	5.04
	(0.06)	(0.37)	(0.33)	(0.67)	(0.54)	(0.17)	(0.14)
1.00	0.37	5.21	5.94	16.98	32.37	8.86	5.36
	(0.05)	(0.34)	(0.58)	(0.65)	(0.74)	(0.16)	(0.20)
1.25	**0.30**	7.37	6.70	22.43	39.91	9.05	5.98
	(0.03)	(0.72)	(0.41)	(1.07)	(0.81)	(0.28)	(0.27)
1.50	0.36	7.23	8.12	25.37	46.71	10.34	6.70
	(0.04)	(0.81)	(0.84)	(0.92)	(1.05)	(0.30)	(0.16)

However the accurate estimation of the 'optimal' value of β is difficult in many cases as the plot of the average misclassification rate against β (see figs 8 to 14) is J-shaped in the area of interest.

TABLE V

Average percentage of black pixels classified white using model III
standard errors in brackets
Optimal reconstruction is bold faced

$\sigma^2=0.5$

β	BCIR	CROSS	TWO	MANY	VMANY	MRF2	MRF3
0.25	6.27	9.37	9.12	12.75	**16.42**	10.91	9.13
	(0.12)	(0.33)	(0.34)	(0.34)	(0.25)	(0.20)	(0.19)
0.50	1.16	4.52	4.81	**11.30**	16.88	8.08	5.33
	(0.06)	(0.37)	(0.19)	(0.37)	(0.36)	(0.21)	(0.16)
0.75	0.49	5.11	4.64	13.05	21.26	**7.74**	**4.98**
	(0.06)	(0.40)	(0.27)	(0.60)	(0.46)	(0.14)	(0.14)
1.00	0.40	**4.82**	**4.48**	14.55	26.60	8.47	5.25
	(0.06)	(0.41)	(0.39)	(0.56)	(0.70)	(0.16)	(0.20)
1.25	**0.35**	6.35	5.63	18.96	32.26	8.62	5.48
	(0.04)	(0.59)	(0.39)	(0.86)	(0.87)	(0.18)	(0.22)
1.50	0.37	6.05	6.05	21.36	39.30	9.67	6.19
	(0.04)	(0.63)	(0.58)	(0.87)	(1.03)	(0.23)	(0.17)

TABLE VI

Average percentage of white pixels classified black using model II
Standard errors in brackets
Optimal reconstruction is bold faced

σ^2=0.5

β	BCIR	CROSS	TWO	MANY	VMANY	MRF2	MRF3
0.25	4.61	4.45	4.60	5.08	7.58	10.22	7.79
	(0.11)	(0.12)	(0.10)	(0.13)	(0.16)	(0.24)	(0.19)
0.50	0.83	0.69	0.80	1.07	3.21	**7.83**	**4.85**
	(0.05)	(0.04)	(0.05)	(0.05)	(0.12)	(0.13)	(0.19)
0.75	**0.64**	**0.55**	**0.53**	0.77	2.22	8.79	5.23
	(0.04)	(0.06)	(0.06)	(0.05)	(0.11)	(0.16)	(0.15)
1.00	0.82	0.58	0.54	0.53	**1.71**	9.16	5.60
	(0.07)	(0.05)	(0.05)	(0.05)	(0.10)	(0.18)	(0.14)
1.25	1.08	0.60	0.71	**0.53**	1.85	10.63	6.35
	(0.10)	(0.07)	(0.10)	(0.05)	(0.18)	(0.28)	(0.25)
1.50	0.95	0.66	0.90	0.60	1.66	10.46	6.85
	(0.07)	(0.05)	(0.08)	(0.05)	(0.10)	(0.27)	(0.16)

TABLE VII

Average percentage of white pixels classified black using model III
Standard errors in brackets
Optimal reconstruction in bold face

σ^2=0.5

β	BCIR	CROSS	TWO	MANY	VMANY	MRF2	MRF3
0.25	6.35	6.25	6.38	6.87	9.17	11.33	9.28
	(0.14)	(0.13)	(0.12)	(0.14)	(0.15)	(0.25)	(0.18)
0.50	1.20	1.06	1.14	1.60	3.93	**7.87**	5.10
	(0.06)	(0.05)	(0.06)	(0.05)	(0.14)	(0.15)	(0.18)
0.75	**0.68**	0.59	0.59	0.91	2.60	8.28	**4.97**
	(0.05)	(0.06)	(0.05)	(0.05)	(0.08)	(0.20)	(0.14)
1.00	0.82	0.58	**0.49**	**0.57**	**1.95**	8.80	5.14
	(0.07)	(0.05)	(0.05)	(0.04)	(0.08)	(0.13)	(0.10)
1.25	0.99	**0.55**	0.64	0.57	2.02	9.89	5.96
	(0.08)	(0.06)	(0.08)	(0.07)	(0.17)	(0.22)	(0.20)
1.50	0.93	0.58	0.80	0.60	1.59	9.78	6.25
	(0.07)	(0.05)	(0.08)	(0.05)	(0.10)	(0.26)	(0.17)

The number of misclassified pixels is a crude image summary which takes no account of the spatial characteristics of the scene. To gain further insight into the differences between model II and III we use an image summary which counts the number of misclassified pixels close to the true boundary between black and white areas. A similar procedure was suggested by Owen, in the discussion of Ripley (1986).

TABLE VIII

Average percentage of misclassified boundary pixels
for MRF3. Standard errors in brackets
The optimal reconstruction in bold face
(There are 2712 boundary pixels in MRF3)

$\sigma^2=0.5$

		β					
Model		0.25	0.50	0.75	1.0	1.25	1.5
II	Boundary	16.74	**16.02** (0.23)	17.35 (0.17)	18.33 (0.21)	20.30 (0.22)	21.42 (0.25)
II	All	7.74	**4.92** (0.12)	5.13 (0.09)	5.48 (0.07)	6.16 (0.08)	6.77 (0.12)
III	Boundary	17.27	**15.98** (0.25)	16.78 (0.18)	17.51 (0.28)	19.11 (0.25)	20.19 (0.20)
III	All	9.20	5.22 (0.12)	**4.98** (0.09)	5.20 (0.10)	5.72 (0.09)	6.22 (0.09)

We reconstruct MRF3 using models II and III with $\sigma^2=0.5$. The average percentage of misclassified boundary pixels are displayed in Table VIII. In this table we call a pixels with at least one neighbour of a different colour (*in the true scene*) a boundary pixel. It is immediately apparent that the majority of misclassified pixels lie near colour boundaries when moderate values of β are used. When MRF3 is reconstructed using model III and $\beta=0.5$ there are approximately 433 misclassified boundary pixels and 89 elsewhere. There is some evidence that the optimal reconstruction of boundary pixels require a smaller value of β than the scene as a whole. This is also apparent from the example described by Owen in the discussion of Ripley (1986). There appears to be little observable difference between Model II and III using this image summary.

5. THE CHOICE OF THE SMOOTHING PARAMETER.

In this section we attempt to identify features of the underlying scene and

error distribution which influence the choice of β in (2.6). We restrict attention to model II. First we examine the relationship between the 'optimal' value of β and the signal variance σ^2. In figures 8 to 14 we plot the average percentage of misclassified pixels against β for various values of σ^2. Notice that the value of β which gives the smallest average misclassification rate is approximately the same for all values of σ^2 considered. The results for VMANY (fig 12) behave atypically. In this respect the ICM algorithm differs from simple linear regularisation techniques where the 'optimal' smoothing parameter is typically proportional to the noise to signal ratio , Hall & Titterington (1986, p 336). The effect of grossly misspecifying σ^2 can be large as the example given in figure 7 of Ripley (1986) shows. However the relative stability of the misclassification rate to changes in β chose to its 'optimal' value suggests that ICM is robust to modest misspecification of σ^2. We see from figs 8 to 14 that worthwhile gains can be achieved using the 'optimal' value of β.

Figs 8-15 *here*

In the remainder of this section we examine the relationship between the 'optimal' value of β and certain features of the underlying scene. First we consider the relationship between the 'optimal' value of β and *its maximum* pseudo-likelihood estimate. In this approach we calculate the value of β which maximises the conditional likelihood

$$\prod_{i=1}^{m}\prod_{j=1}^{n} P(x_{ij} \mid F_{(i,j)}, \beta). \tag{5.1}$$

From Table IX we see that the pseudo-likelihood estimates of β using model II (β_{lik}) are usually greater that the value of β giving the smallest average misclassification rate. This behaviour may be due to the fact that the majority of scenes considered are untypical realisations from a MRF. For the scenes constructed by sampling from a *conditional* MRF a different pattern emerges. In this case the 'optimal' β is precisely the value of β used to construct the underlying scene (see Tables II,III and IX), **provided we use the correct model in our reconstruction**. The pseudo-likelihood approach has the

disadvantage of indicating an infinite value of β for certain pixel configurations.

Next we introduce two statistics which measure the smoothness of the underlying scene.

DEFINITION : TWO IMAGE SUMMARIES

B : *Total boundary length between black and white pixels (excluding the window).*

Q_{T_i} : *The number of pixels which have at least one neighbour of a different colour using an i^{th} order neighbourhood.*

Notice that Switzer (1976) measures the 'smoothness' of a random function by the total arc length of its contour plot at certain levels. Applying this measure to binary random functions gives the statistic B. The image summary Q_{T_i} can be written as the difference between the statistics e_t and d_t defined in Ripley (1986, p 94) where pixels adjacent to the window are neglected. See Ripley (1977) for a discussion of image summaries and their application. Notice that $Q_{T_2} = 2B$ for many scenes (see Table IX for several examples). These statistics differ in their treatment of 'small' features. An isolated black pixel will contribute 4 to the total boundary length and 9 to Q_{T_2}.

There is strong evidence (see Table IX) to suggest that the misclassification rate for a feature is strongly influenced by the percentage of boundary pixels (as measured by Q_{T_2} or boundary length, B). This effect is indicated by the difference in the average percentage of misclassified black and white pixels. The scene BCIR appears to behave in an anomalous way. There is some evidence (see Table IX) that the value of β giving the lowest average proportion of misclassified pixels decreases as the proportion of boundary pixels (as

measured by Q_{T_2} or total boundary length) increases. The value of β giving the smallest average percentage of misclassified pixels gives the strongest evidence for this relationship. There appears to be little difference in the descriptive ability of Q_{T_2} and B. In the scenes considered we see that the pseudo-likelihood estimates of β are not closely related to the smoothness measures described above.

TABLE IX

Smallest average percentage of misclassified pixels using model II and the 'optimal' value of β vs smoothness measures.
(* pseudo likelihood estimate using model III)

$\sigma^2 = 0.5$

Picture	black	white	all	Q_{T_2}	B	β_{lik}
BCIR	0.30	0.64	0.55			
β	1.25	0.75	0.75	344	172	1.85
pixels	4300	5700	10000			
CROSS	4.30	0.55	1.00			
β	0.50	0.75	0.75	516	260	2.09
pixels	926	9074	10000			
TWO	4.87	0.53	1.11			
β	0.5	0.75	0.75	480	240	2.12
pixels	1225	8775	10000			
MANY	11.91	0.53	2.41			
β	0.25	1.25	0.5	1248	624	2.62
pixels	1216	8784	10000			
VMANY	16.16	1.71	7.11			
β	0.25	1.0	0.5	3776	1888	1.98
pixels	2560	7440				
MRF2	7.87	7.83	7.85	4109	2324	0.50
β	0.5	0.5	0.5			
pixels	5065	4935				
MRF3	4.98	4.85	4.92	2712	1453	0.63
β	0.5	0.5	0.5			(* 0.75)
pixels	5065	4935				

A useful indication of the effectiveness of a reconstruction technique can be obtained by considering its properties in reconstructing a one colour scene. In

Table X we display the average percentage of misclassified pixels when a one colour scene is reconstructed using model II. For values of β less that 0.4 appreciable errors are incurred. So for scenes with large monochrome areas we should choose $\beta \geq 0.4$.

TABLE X

Average percentage of misclassified pixels for a one colour scene (using model II) for various values of σ^2
Standard error in brackets

β	0.2	0.25	0.3	0.35	0.4
$\sigma^2 = 0.25$	4.98 (0.03)	3.35 (0.03)	2.15 (0.02)	1.30 (0.02)	0.80 (0.01)
$\sigma^2 = 0.50$	6.6 (0.06)	3.93 (0.05)	2.26 (0.03)	1.31 (0.03)	0.75 (0.02)
$\sigma^2 = 0.75$	7.14 (0.06)	4.06 (0.06)	2.34 (0.05)	1.40 (0.04)	0.82 (0.03)
$\sigma^2 = 1.0$	7.24 (0.08)	4.25 (0.07)	2.61 (0.06)	1.59 (0.05)	1.06 (0.05)
$\sigma^2 = 1.25$	7.49 (0.08)	4.46 (0.09)	2.68 (0.07)	1.87 (0.07)	1.31 (0.06)
$\sigma^2 = 1.50$	7.68 (0.10)	4.52 (0.09)	3.03 (0.08)	2.11 (0.08)	1.52 (0.05)

To illustrate this point further consider the percentage of misclassified pixels for BCIR with σ^2=0.25. Recall that the majority of pixels in BCIR are far from the colour boundaries. In Figure XI we compare the percentage of misclassified pixels using ICM with the percentage of misclassified pixels for a one colour scene using the same model.

TABLE XI

A comparison of the average percentage of misclassified pixels of BCIR
and a monochrome scene when reconstructed using model II
Standard errors in brackets (60 realisations for mono scene)
Optimal reconstruction is bold faced

σ^2=0.25

	β					
	0.25	0.50	0.75	1.00	1.25	1.50
BCIR	4.53	0.80	**0.55**	0.65	0.75	0.70
	(0.10)	(0.03)	(0.04)	(0.04)	(0.04)	(0.03)
Monochrome	3.34	0.27	**0.02**	<0.02	<0.02	<0.02
	(0.02)	(0.01)	(0.003)	(<0.001)	(<0.001)	(<0.001)

The optimal reconstruction is obtained with β=0.75, where the percentage of misclassified pixels is 0.55. The contribution of pixels far from the colour boundary is approximately 0.02%. These result suggest that the errors incurred during the reconstruction of scenes like BCIR occur near the colour boundaries for moderate values of β (see Table VIII).

Consider a black pixel which has k white neighbours when it is updated. The probability of misclassifying this pixel during the *current iteration* can be calculated from (2.6). In Table XII we display this probability for model II with independent normally distributed noise (σ^2=0.5).

TABLE XII

The probability that a black pixel is classified white
at a *particular iteration* when it has k white neighbours

σ^2=0.5

		β	
k	0.25	0.50	1.0
8	0.98	1.00	1.00
7	0.92	1.00	1.00
6	0.76	0.98	1.00
5	0.50	0.76	0.98
4	0.16	0.16	0.16
3	0.08	0.02	0.00
2	0.02	0.00	0.00
1	0.00	0.00	0.00
0	0.00	0.00	0.00

These calculations strongly suggest that model II behaves like a simple majority

vote when $\beta \geq 1.0$. Table XII can be used to estimate the 'vulnerability' of image features for various values of β. As an example consider the corner pixels (k=5) of a black rectangle. This configuration is highly vulnerable when $\beta \geq 0.5$. As ICM is an iterative procedure this calculation will not give the probability of misclassifying a given pixel. However calculations of this type are useful in visualising the effect of ICM with various values of β and neighbourhood system. Using this approach to choose β is analogous to a method suggested by Ripley (1986) with the important addition, that information is included about the noise distribution.

6. SOME DISTRIBUTIONAL PROPERTIES OF ICM

There appears to be no work in the literature on the distributional properties of the ICM estimator of (x_{ij}) or any functional of interest. The only relevant work is due to Geman and Geman (1984), who describe how to sample from the posterior distribution of (x_{ij}). In this section we examine the variance of the percentage of misclassified pixels. The number of misclassified pixels can be regarded as a functional of the scene formed by a comparison between (x_{ij}) and its reconstruction. In Table XIII we display the average percentage of misclassified pixels with its standard deviation in brackets for $\sigma^2=0.5$ and model II. The figures for the optimal reconstruction are given in bold face. Recall that ICM is a 'local' procedure. This suggests a poisson approximation for the number of misclassified pixels. The coefficient of variation of the percentage of misclassified pixels at the 'optimal' value of β appears to decrease as the misclassification rate (and complexity) increases. This is not consistent with a poisson assumption. In particular we see from Table VIII that misclassified pixels cluster near colour boundaries. The skewness $(b_1^{1/2})$ and kurtosis (b_2) of the percentage of misclassified pixels were calculated and suggest a symmetric distribution with b_2 between two and three. These are

tentative conclusions as the number of realisations used in this study is small.

TABLE XIII

The standard deviation (in brackets) and the average percentage of misclassified pixels using model II
The optimal reconstruction is bold faced

σ^2=0.5

β	BCIR	CROSS	TWO	MANY	VMANY	MRF2	MRF3
0.25	4.53 (0.40)	4.75 (0.42)	4.96 (0.33)	5.91 (0.49)	9.78 (0.34)	9.86 (0.54)	7.74 (0.48)
0.50	0.80 (0.10)	1.02 (0.16)	1.30 (0.17)	**2.41** **(0.29)**	**7.11** **(0.39)**	**7.85** **(0.35)**	**4.92** **(0.33)**
0.75	**0.55** **(0.14)**	**1.00** **(0.26)**	**1.11** **(0.18)**	2.48 (0.34)	8.04 (0.73)	8.44 (0.39)	5.13 (0.25)
1.00	0.63 (0.16)	1.01 (0.20)	1.20 (0.25)	2.53 (0.35)	9.56 (0.71)	9.01 (0.35)	5.48 (0.32)
1.25	0.75 (0.21)	1.22 (0.33)	1.44 (0.38)	3.19 (0.41)	11.60 (0.96)	9.83 (0.45)	6.16 (0.47)
1.50	0.70 (0.12)	1.27 (0.33)	1.78 (0.46)	3.61 (0.46)	13.19 (1.10)	10.40 (0.51)	6.77 (0.45)

7. COMPUTATIONAL DETAILS

Pseudo-random deviates distributed uniformly on [0,1] were generated using Wichmann & Hill (1982). We take ix=27631 , iy=5627 and iz=10234. Pseudo-normal deviates with zero mean and unit variance were constructed using the Box-Muller transformation. The first step in our algorithm is to determine the maximum likelihood estimate of (x_{ij}). This colouring is used as the initial state (iteration zero) of our algorithm. Each pixel is visited in raster scan order and the colour of the $(i,j)^{th}$ pixel is updated using (2.6). The cpu time taken by our algorithm is proportional to the size of the neighbourhood system used, the number of pixels and the size of σ^2.

In Table XIV we display the average number of pixels whose colour changes during the k^{th} iteration when MRF3 is reconstructed using model II.

The average percentage of misclassified pixels is also presented. In this table one iteration is equivalent to a complete sweep of the scene (10^4 pixel visits).

Notice that the majority of changes occur during the first iteration (more changes are made as β increases). Typically only one or two pixels change colour during later iterations. This pattern is repeated for each combination of scene, σ^2 and model considered.

TABLE XIV

Average number of changes per iteration and percentage of misclassified pixels for MRF3 (model II)
Standard errors in brackets

$\sigma^2=0.5$

	$\beta=0.25$		$\beta=0.50$		$\beta=1.0$	
k	changes	% miscl'd	changes	% miscl'd	changes	%miscl'd
1	1587 (8)	9.84 (0.13)	2117 (12)	6.47 (0.09)	2346 (10)	6.58 (0.08)
2	206 (5)	8.18 (0.12)	189 (4)	5.31 (0.08)	153 (3)	5.93 (0.08)
3	42 (2)	7.87 (0.12)	44 (3)	5.07 (0.08)	50.0 (2)	5.70 (0.08)
4	12 (1)	7.78 (0.12)	16 (1)	4.98 (0.08)	21 (1)	5.58 (0.08)
5	3 (1)	7.75 (0.12)	6 (1)	4.95 (0.08)	10 (1)	5.52 (0.08)
6	1 (0)	7.74 (0.12)	3 (0.6)	4.93 (0.08)	5 (1)	5.50 (0.08)
12	0	7.74 (0.12)	0	4.92 (0.09)	0	5.48 (0.08)

This suggests the following modification of the basic algorithm:

Pixels are only updated when they are flagged as 'active'. The pixel (i,j) is 'active' when the colour of at least one of neighbours has changed during the current iteration. Pixels are visited in raster order. When a pixel's colour

changes its neighbours become active. Pixels are de-activated after they are updated.

Using this algorithm we would visit (see Table XIV) less than nine hundred pixels on average (using a second order neighbourhood) during the third iteration. We expect the modified algorithm to converge after approximately 3 iterations in general. To obtain further gains in efficiency we might 'switch off' pixels whose colour has a low probability of being changed during the current iteration,see Ripley (1986). For example a pixel which has no neighbours of a different colour can be de-activated.

8. CONCLUSIONS

On the basis of the scenes and models considered in this study we suggest the following rules of thumb for prospective users of ICM.

1. Should I use ICM ?

Our empirical results suggest that the misclassification rate of a feature increases with the proportion of boundary pixels (see Table IX and compare the misclassification rate for black and white pixels). Typically small feature will be 'erased'. If the aim of an analysis is to find small features then a technique based on masks will probably be preferable to ICM. However it is apparent from Table I that substantial gains over the maximum likelihood estimate, can be achieved by smoothing.

2. Which model should I use?

We suggest that model III should be used in the absence of specific knowledge about the uncorrupted scene. If we know that the underlying scene

is non-homogeneous we can exploit this by using a hierarchical model, see Derin & Elliot (1987) or Woods,Dravida & Mediavilla (1987).

3. What value of β *should I use?*

This is a difficult question to answer in the absence of any information about the underlying scene. The examples considered in this paper suggest that useful gains can be achieved using the 'optimal' value of β rather than a portmanteau value of , say β=1.5. We distinguish between two cases. In the first we assume that the underlying scene is a 'typical' realisation from a MRF. Then a good approximation to the 'optimal' reconstruction is obtained using the neighbourhood system and value of β specified by the underlying MRF. When the underlying scene cannot be regarded as a 'typical' realisation from a MRF we suggest the used of smoothness measures such as the total boundary length in the choice of the 'optimal' value of β. In both cases we see that the 'optimal' value of β does not depend on σ^2. From figs 8 to 14 we see that there is some leeway in choosing the 'optimal' value of β.

4. Is the ICM estimate difficult to calculate?

From the discussions in section 7 we see that a single reconstruction of a binary 10^4 pixel scene can be computed simply. The calculations appear well suited to parallel implementation. The scene VMANY with σ^2=0.5 was reconstructed in around 39 seconds (using model II with β=0.5) on a SUN-3 Work Station with a floating point accelerator.

Acknowledgement

I would like to thank Dr. C. Jennison and Professor B.W. Silverman for their helpful comments during the course of this work. The financial support of

the European Research Office of the U.S. Army is gratefully acknowledged.

References

Besag, J. (1974). Spatial interaction and the statistical analysis of lattice systems (with Discussion). *J.Roy. Statist. Soc. Ser. B* **36,** 192-236.

Besag,J. (1986). On the statistical analysis of dirty pictures (with Discussion). *J. Roy. Statist. Soc. Ser. B* **48** , 259 - 302.

Bovik, A.C. , Huang, T.S. & Munson, D.C. (1987). The effect of median filtering on edge estimation and detection. *I.E.E.E. Trans. Pattern Anal. Machine Intell.* **9** , 181 - 194.

Brown,T.C. & Silverman, B.W. (1987). Edge process models for regular and irregular pixels. *Technical report no. 267. Stanford University.*

Cross, G.R. & Jain, A.K. (1983). Markov random field texture models. *I.E.E.E. Trans. Pattern Anal. Machine Intell.* **5**, 25 - 39.

Derin,H. & Elliot, H. (1987). Modeling and segmentation of noisy and textured images using Gibbs random fields. *I.E.E.E Trans. Pattern Anal. Machine Anal. Intell.* **6** , 39 - 55.

Enting, I.G. & Welberry, T.R. (1978). Connections between Ising models and various probability distributions. *Suppl. Adv. in. Appl. Probab.* **10,** 65 - 72.

Geman, S. & Geman, D. (1984). Stochastic relaxation, Gibbs distributions, and the Bayesian restoration of images. *I.E.E.E. Trans. Pattern Anal. Machine Intell.* **6**, 721 - 741.

Hall, P. & Titterington, D.M. (1986). On some smoothing techniques used in image restoration. *J.R. Statist. Soc. Ser B* **48** , 330 - 343.

Kashyap, R.L. & Chelappa, R. (1983). Estimation and choice of neighbors in spatial interaction models of images. *I.E.E.E. Trans. Inform. Theory* **29** , 60 - 72.

Kashyap, R.L. & Lapsa, P.M. (1984). Synthesis and estimation of random fields using long correlation models. *I.E.E.E. Trans. Pattcrn Anal. Machine Intell.* **6** , 800 - 809.

Van Laarhoven, P.J.M & Aaris, E.H.L. (1987). *Simulated Annealing: Theory and Applications*. D.Reidel Publishing Company.

Marroquin, J. , Mitter, S. and Poggio, T. (1987). Probabilistic solution of ill-posed problems in computational vision. *J. Amer. Statist. Assoc.* **82** , 76 - 89.

Pickard, D.K. (1987). Inference for discrete markov fields: The simplest non-trivial case. *J. Amer. Statist. Assoc.* **82** , 90 - 96.

Ripley, B.D. (1977). Modelling spatial patterns. *J. Roy. Statist. Soc. Ser. B* **39** , 172 - 212.

Ripley, B.D. (1984). Spatial Statistics.Developments 1980-3. *Internat. Statist. Rev.* **53** , 141-150.

Ripley, B.D. (1986). Statistics,images and pattern recognition. *Canad. J. Statist.* **14** , 83 - 111.

Rosenfeld, A. and Kak, A.C. (1982). *Digital Picture Processing*. Academic Press,Orlando.

Serra, J. (1982). *Image Analysis and Mathematical Morphology*. Academic Press, London.

O'Sullivan, F. (1986). A Statistical perspective on ill-posed problems (with discussion). *Statist. Sci.* **1** , 502 - 527.

Switzer, P. (1976). Geometrical measures of the smoothness of random functions. *J. Appl. Probab.* **13** , 86 - 95.

Suomela, P. (1976). Construction of nearest neighbour systems. *Annales Academiae Scientiarum Fennicae. Series A. Mathematica Dissertationes* **10.**

Titterington, D.M. (1985). Common structure of smoothing techniques in statistics. *Internat. Statist. Rev.* **53** , 141-170.

Wichmann, B.A. & Hill, I.D. (1982). Algorithm AS 183. An efficient and portable pseudo-random number generator. *J. Roy. Statist. Soc. Ser. C* **31** ,188-190.

Wolberg, G. & Pavlidis, T. (1985). Restoration of binary images using stochastic relaxation with annealing. *Pattern Recognition Letters.* **3** , 375 - 388.

Woods,J.W. , Dravida, S. & Mediavilla, R. (1987). Image estimation using doubly stochastic Gaussian random field models. *I.E.E.E. Trans. Pattern Anal. Machine Intell.* **9** , 245 - 253.

CAPTIONS FOR FIGURES 1 TO 15

FIGURE 1 BCIR : Circle centred at (30,30) with radius 40. The origin is at the bottom left hand corner of the window which has dimensions (0,100)x(0,100).

FIGURE 2 CROSS : Two rectangles with corners at {(10,40),(60,20),(70,30),(20,50)} and {(25,20),(30,15),(55,50),(50,55)}

FIGURE 3 TWO : Two rectangles with corners at {(10,40) , (60,40) , (60,50) , (10,50)} and {(20,55) , (65,55) , (65,60) , (20,60)}

FIGURE 4 MANY : Eight circles of radius 6 centred at , (25,20) , (45,20) , (65,20) , (80,20) , (25,80) , (45,80) , (65,80) , (85,80) and ten circles of radius 3 centred at (20,40) , (35,40) , (50,40) , (65,40) , (80,40) , (20,60) , (35,60) , (50,60) , (65,60) , (80,60).

FIGURE 5 VMANY : Eighty circles with radius 3 and centres at $(5+10j, 10k-7)$ for $j=1,\ldots,8$ and $k=1,\ldots,10$.

FIGURE 6 MRF2 : A synthetic realisation from the MRF specified in MODEL II with $\beta=0.5$. This scene was constructed using an algorithm given in Cross and Jain (1983).

FIGURE 7 MRF3 : A synthetic realisation from the MRF specified in Model III with $\beta=0.75$. This scene was constructed using the algorithm given in Cross and Jain (1983).

FIGURE 8 A plot of the average percentage of misclassified pixels against β and σ^2 when BCIR is reconstructed using MODEL II

FIGURE 9 A plot of the average percentage of misclassified pixels against β and σ when CROSS is reconstructed using MODEL II

FIGURE 10 A plot of the average percentage of misclassified pixels against β and σ when TWO is reconstructed using MODEL II

FIGURE 11 A plot of the average percentage of misclassified pixels against β and σ when MANY is reconstructed using MODEL II

FIGURE 12 A plot of the average percentage of misclassified pixels against β and σ when VMANY is reconstructed using MODEL II

FIGURE 13 A plot of the average percentage of misclassified pixels against β and σ when MRF2 is reconstructed using MODEL II

FIGURE 14 A plot of the average percentage of misclassified pixels against β and σ when MRF3 is reconstructed using MODEL II

FIGURE 15 A plot of the average percentage of misclassified pixels against β for model II and $(1/1.117)\beta$ for model III

R.H.Glendinning : FIGURE 1

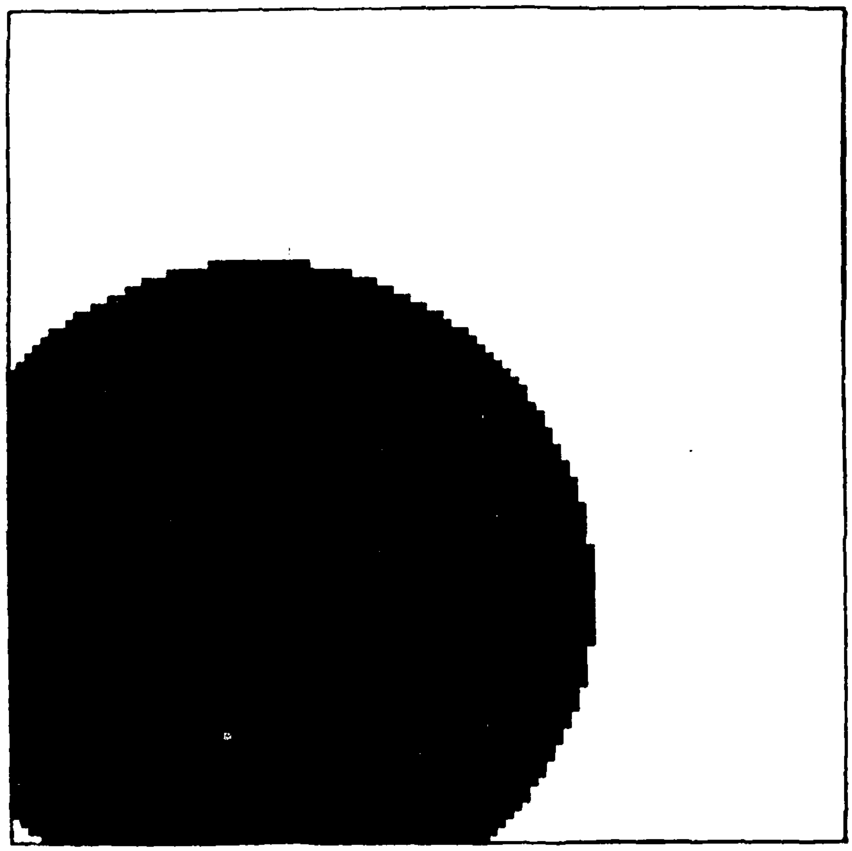

R.H.Glendinning : FIGURE 2

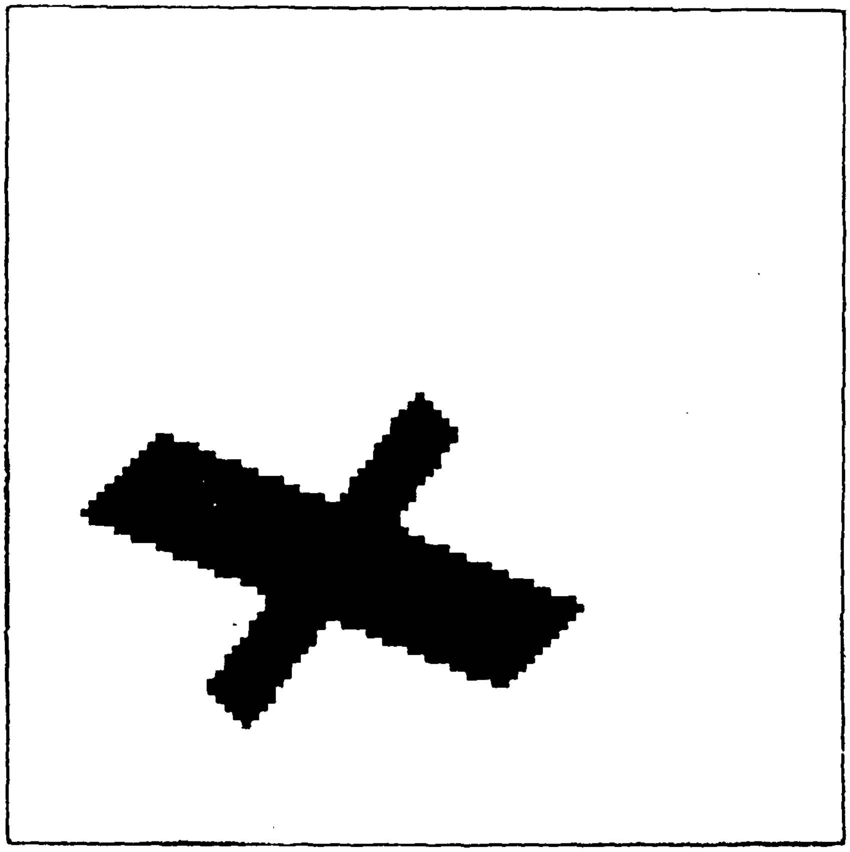

R.H.Glendinning : FIGURE 3

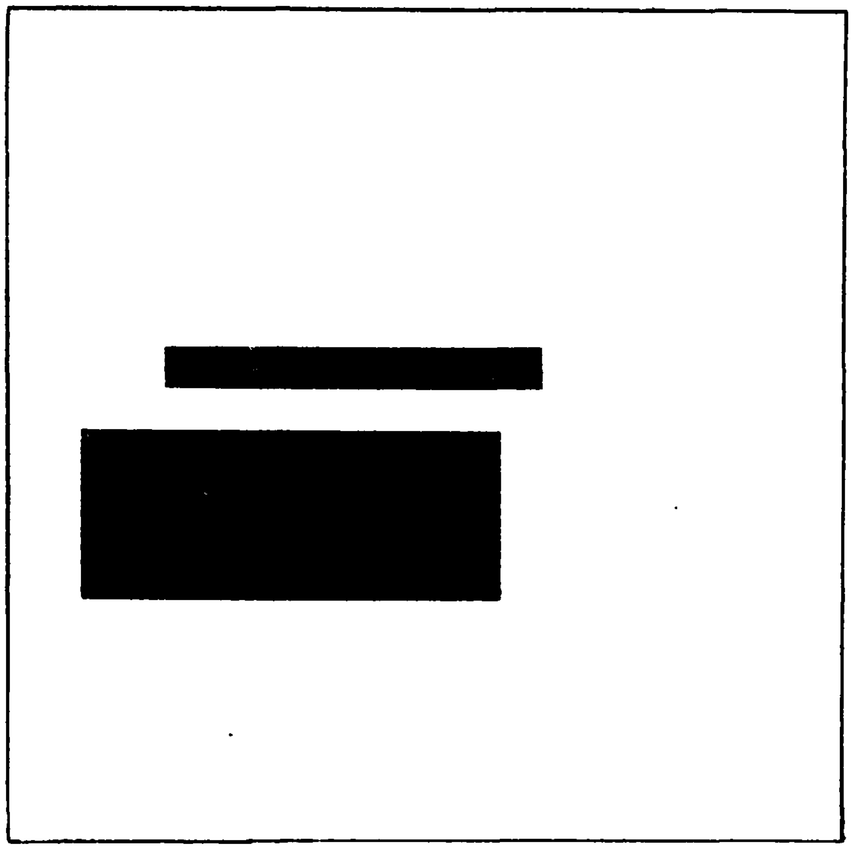

R.H.Glendinning : FIGURE 4

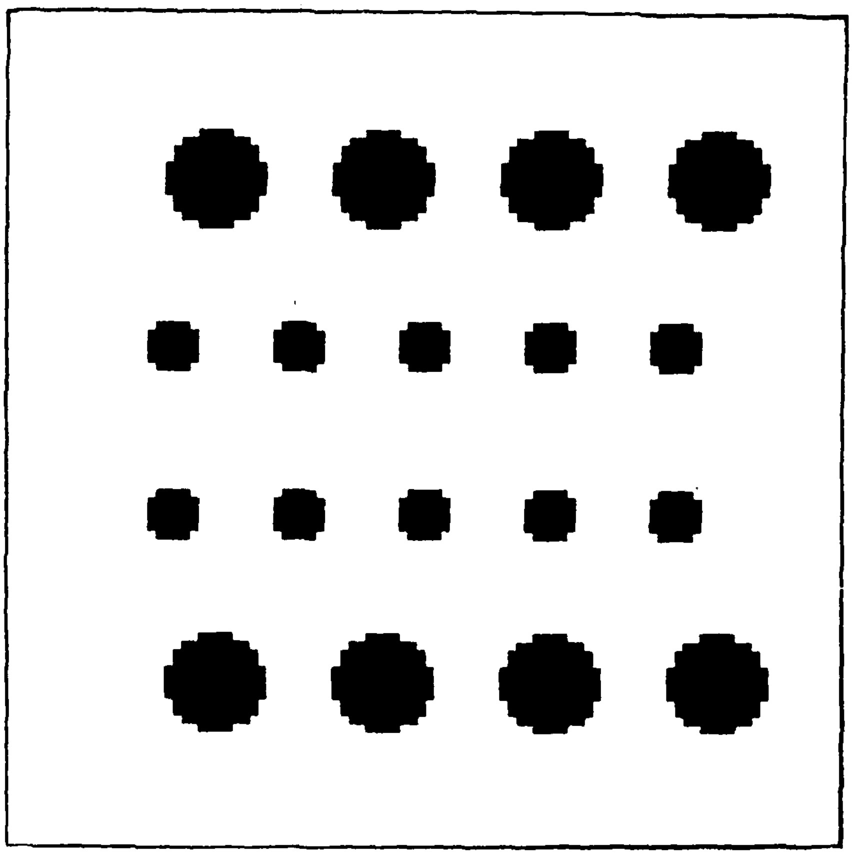

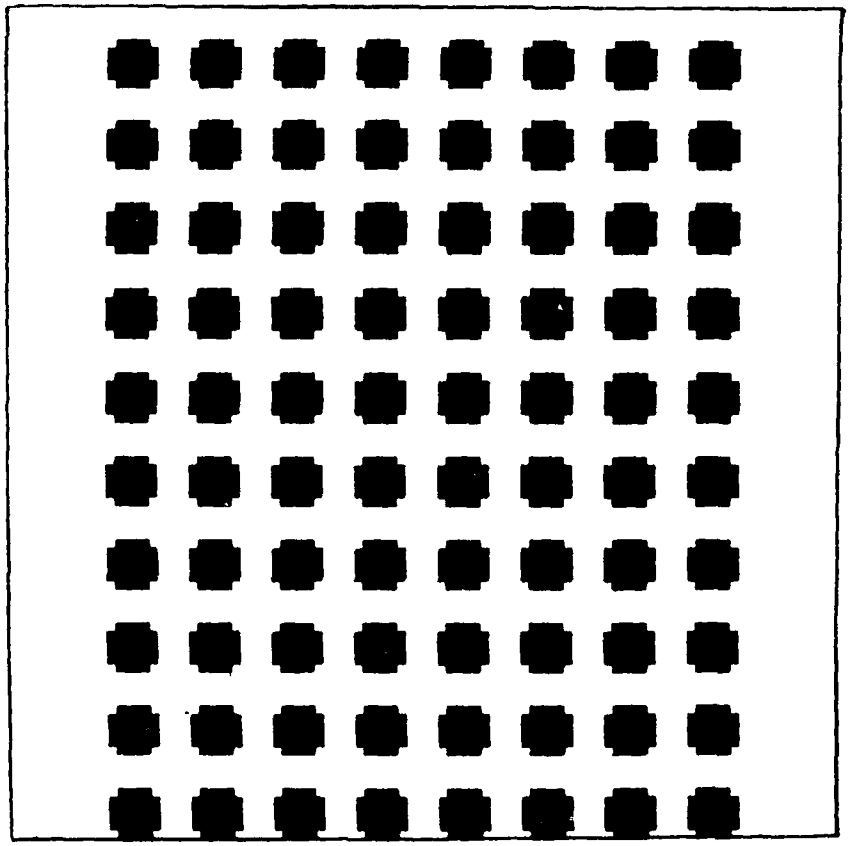

R.H.Glendinning : FIGURE 6

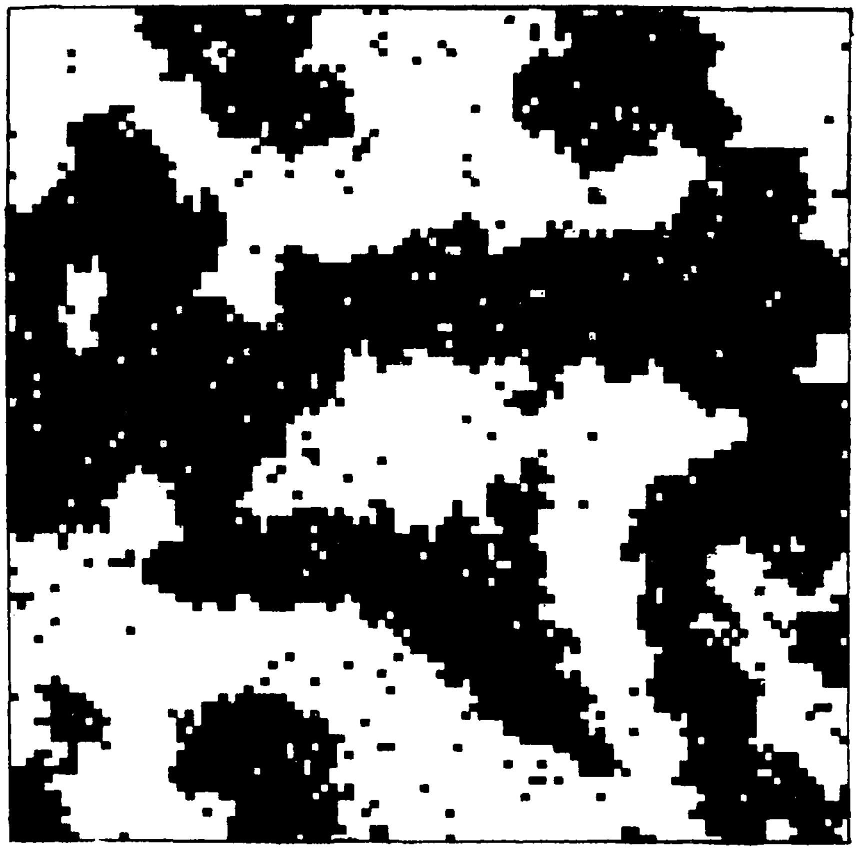

R.H.Glendinning : FIGURE 7

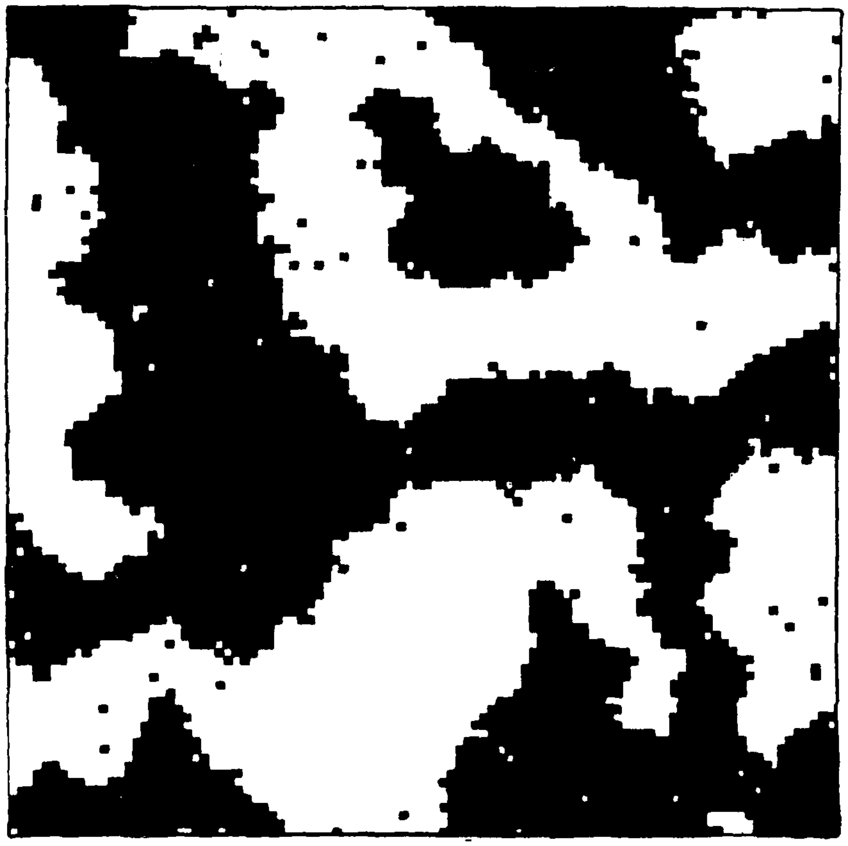

R.H.Glendinning : FIGURE 8

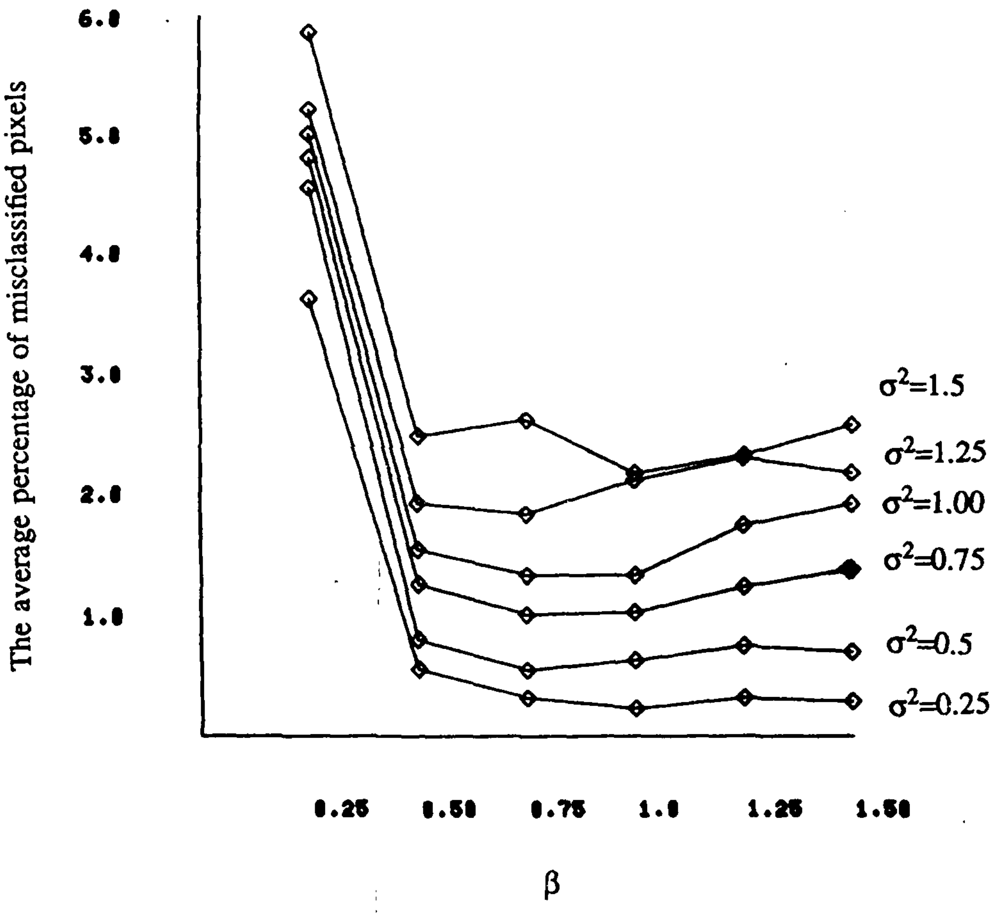

R.H.Glendinning : FIGURE 9

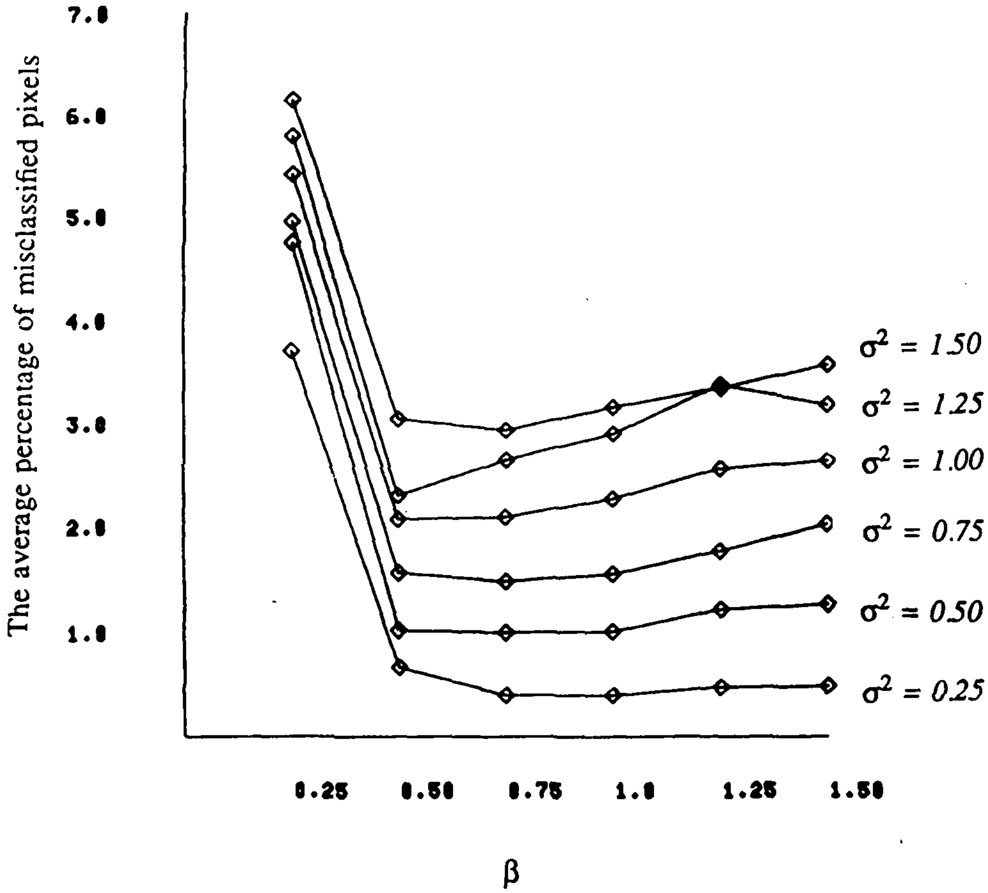

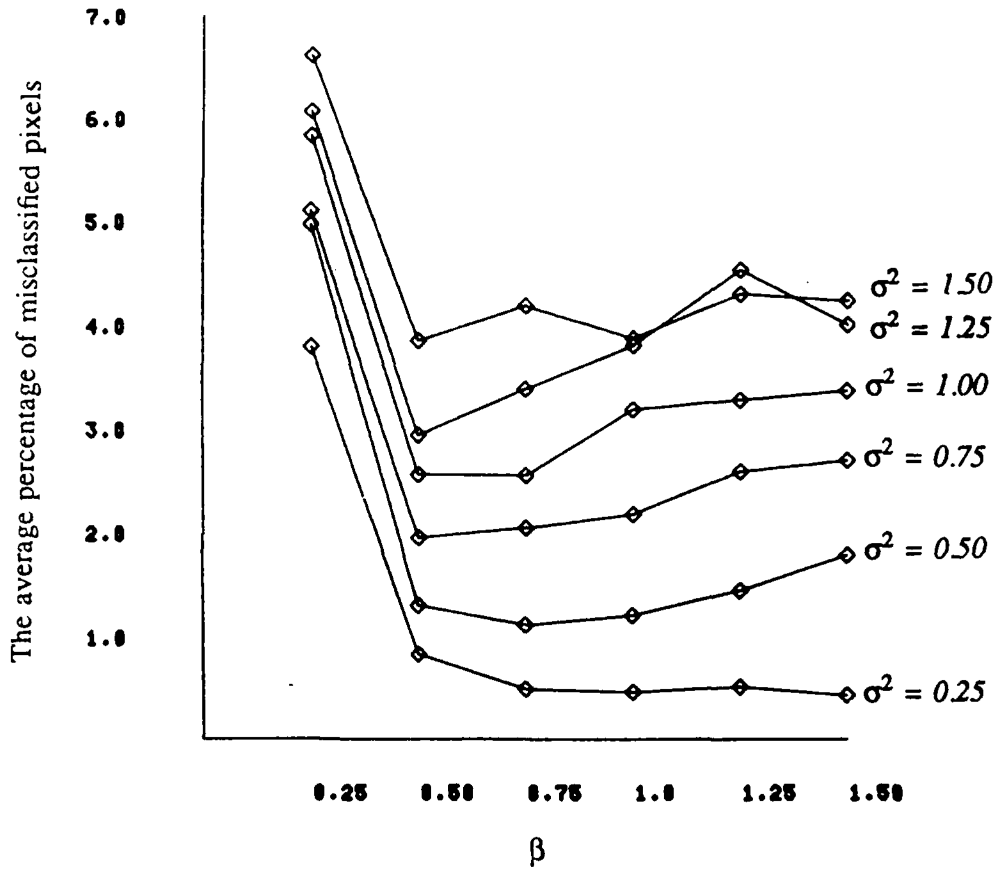
7.0
6.0
5.0
4.0
3.0
2.0
1.0
The average percentage of misclassified pixels
$\sigma^2 = 1.50$
$\sigma^2 = 1.25$
$\sigma^2 = 1.00$
$\sigma^2 = 0.75$
$\sigma^2 = 0.50$
$\sigma^2 = 0.25$
0.25
0.50
0.75
1.0
1.25
1.50
β

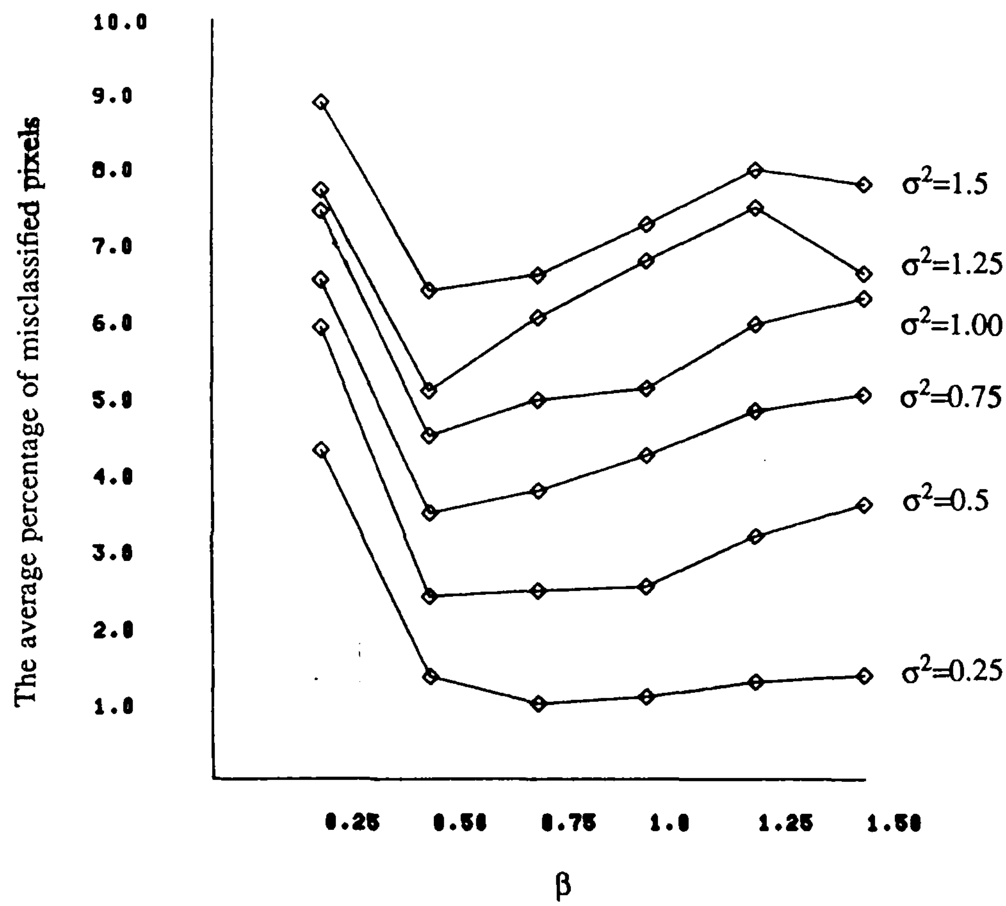
The average percentage of misclassified pixels
10.0
9.0
8.0
7.0
6.0
5.0
4.0
3.0
2.0
1.0
0.25
0.50
0.75
1.0
1.25
1.50
β
σ2=1.5
σ2=1.25
σ2=1.00
σ2=0.75
σ2=0.5
σ2=0.25

R.H.Glendinning : FIGURE 12

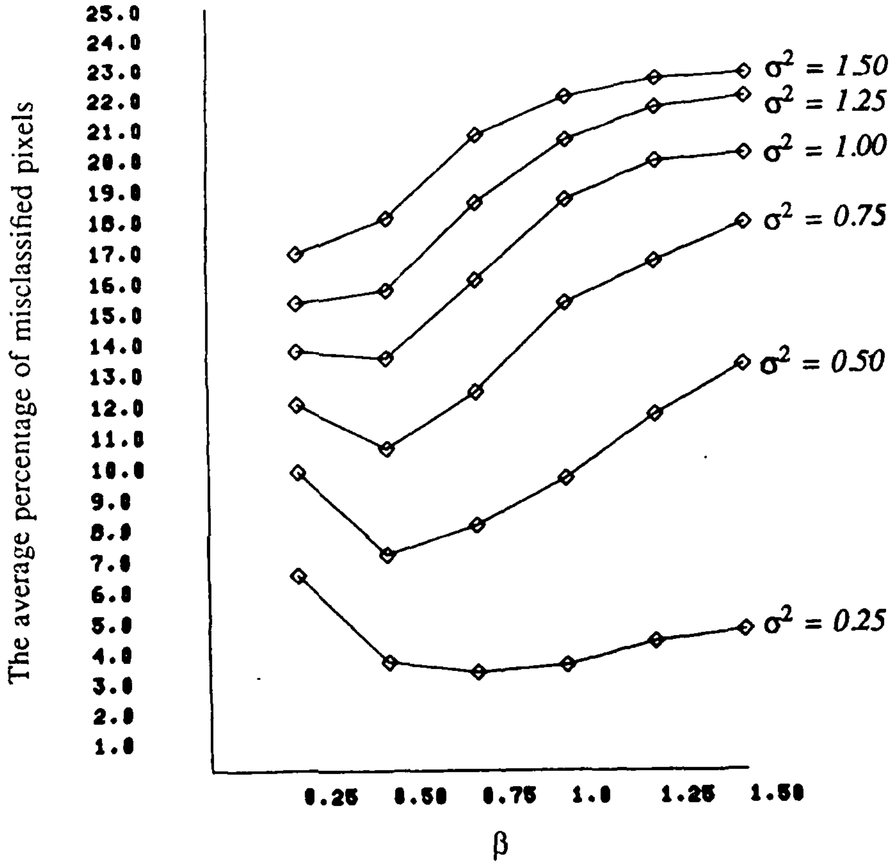

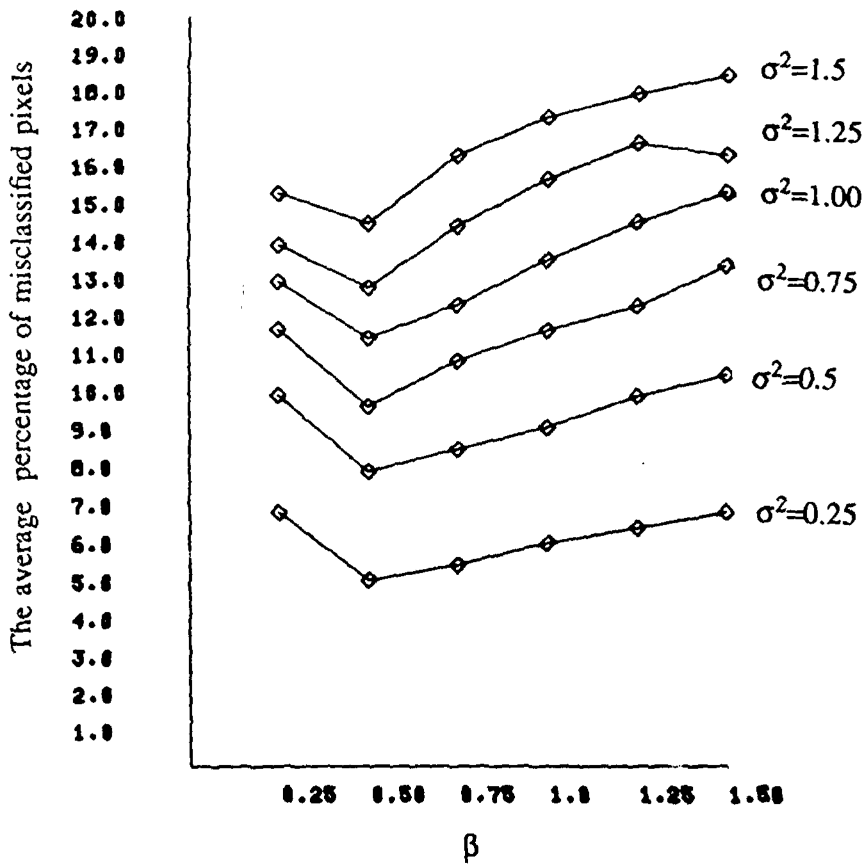
20.0
19.0
18.0
17.0
16.0
15.0
14.0
13.0
12.0
11.0
10.0
9.0
8.0
7.0
6.0
5.0
4.0
3.0
2.0
1.0
The average percentage of misclassified pixels
σ^2=1.5
σ^2=1.25
σ^2=1.00
σ^2=0.75
σ^2=0.5
σ^2=0.25
0.25
0.50
0.75
1.0
1.25
1.50
β

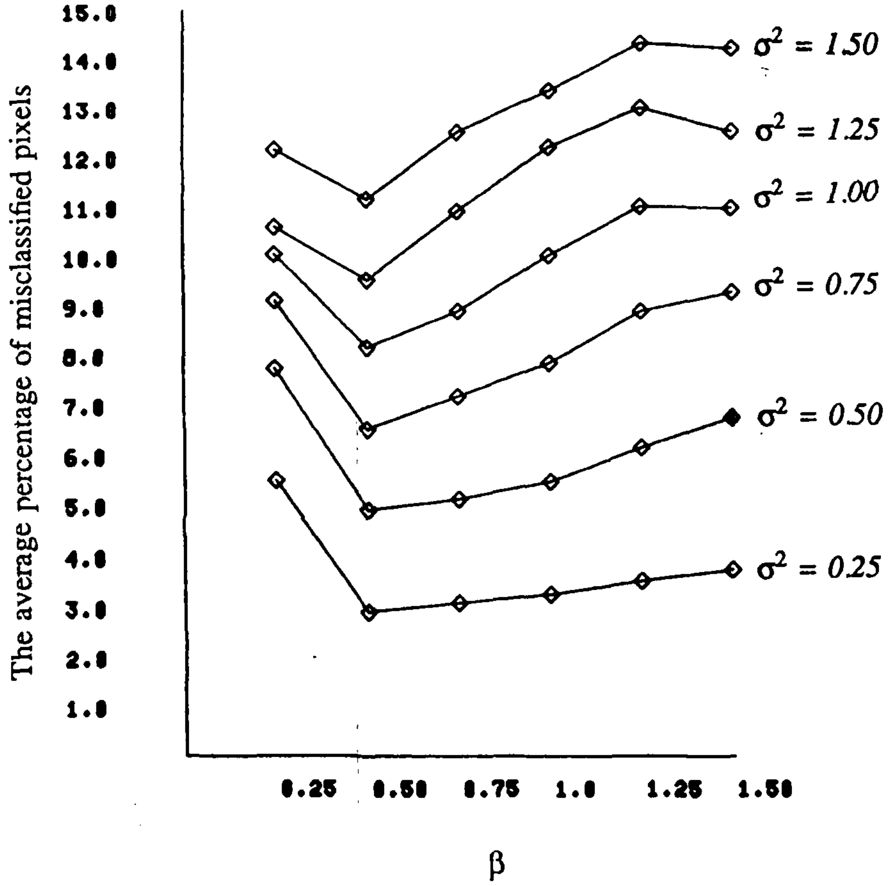
15.0
14.0
13.0
12.0
11.0
10.0
9.0
8.0
7.0
6.0
5.0
4.0
3.0
2.0
1.0
The average percentage of misclassified pixels
0.25
0.50
0.75
1.0
1.25
1.50
β
σ² = 1.50
σ² = 1.25
σ² = 1.00
σ² = 0.75
σ² = 0.50
σ² = 0.25

R.H.Glendinning : FIGURE 15